

# The creep and thermal stability characteristics of a unidirectionally solidified $\text{Al}_2\text{O}_3/\text{YAG}$ eutectic composite

YOSHIHARU WAKU, NARIHITO NAKAGAWA, TAKUMI WAKAMOTO, HIDEKI OHTSUBO, KAZUTOSHI SHIMIZU, YASUHIKO KOHTOKU  
*Ube Research Laboratory, Corporate Research & Development, UBE Industries, Ltd., Ube City, Yamaguchi, 755, Japan*  
*E-mail: 25222u@ube-ind.co.jp*

Compressive creep characteristics at 1773, 1873, and 1973 K, oxidation resistance over 1000 h at a temperature of 1973 K in ambient air, and the thermal stability characteristics at 1973 K in ambient air of a unidirectionally solidified  $\text{Al}_2\text{O}_3/\text{YAG}$  eutectic composite were evaluated. At a test temperature of 1873 K and a strain rate of  $10^{-4}/\text{s}$ , the compressive creep strength of a eutectic composite manufactured by the unidirectional solidification method is approximately 13 times higher than that of a sintered composite with the same chemical composition. The insite eutectic composite also showed greater thermal stability, with no change in mass after an exposure of 1000 hours at 1973 K in ambient air. The superior high-temperature characteristics are closely related to such factors as (1) the in-situ eutectic composite having a microstructure, in which single crystal  $\text{Al}_2\text{O}_3$  and single crystal YAG are three-dimensionally and continuously connected and finely entangled without grain boundaries and (2) no amorphous phase is formed at the interface between the  $\text{Al}_2\text{O}_3$  and the YAG phases. © 1998 Kluwer Academic Publishers

## 1. Introduction

To help solve environmental problems, it is vital to develop a material that can save energy and curb the emission of pollutants such as  $\text{CO}_2$  and  $\text{NO}_x$ . In the advanced power generator field, studies all over the world are seeking to develop ultra-high-temperature structural materials that will improve thermal efficiency in aircraft engines and high-efficiency gas turbines. A 1% improvement of thermal efficiency would lead to a world-wide annual saving in energy costs of around \$1000billion [1], and research is being vigorously pursued into the development of ultra-high-temperature structural materials that remain stable under use for prolonged periods in an oxidizing atmosphere at temperatures above 1923 K [2]. In other words, these materials must be suitable for use as non-cooled turbine blades. Such materials must offer a performance balance in such areas as high-temperature strength, oxidation resistance, creep resistance, fatigue resistance, thermal shock characteristics, and fracture toughness [2].

Ceramics and ceramic-matrix composites hold promise as structural materials with excellent heat resistance, oxidation resistance, and abrasion resistance, and are therefore being researched and developed on a global scale. However, the strength of nearly all ceramic polycrystalline materials drops off rapidly with increases in temperature. According to Hillig [3], the strength in brittle materials should decrease proportionally to  $T/T_m^{3/2}$ , where  $T_m$  is the melting temperature. At

$0.5 T_m$ , the strength is around half that at room temperature because at high temperatures, diffusional processes at grain boundaries, which lead to plastic deformation, play a large role [2, 3].

Keeping in mind the above conditions, the realization of ultra-high-temperature heat-resistant structural materials that remain stable and able to be used for long periods in an air atmosphere requires the development of a new concept material. For this, we believe that the material must be a composite with these characteristics, single-crystal, oxides, thermodynamically stable interfaces and phases, three-dimensionally linked and reinforced phases and matrices.

Viechnicki *et al.* [4] conducted microstructural studies on a  $\text{Al}_2\text{O}_3/\text{Y}_3\text{Al}_5\text{O}_{12}$  (YAG) system using the Bridgman method, and showed that microstructure of the eutectic composite could be controlled by unidirectional solidification. In addition, it has recently been reported that a unidirectionally solidified  $\text{Al}_2\text{O}_3/\text{YAG}$  eutectic composite has superior flexural strength, thermal stability and creep resistance at high temperatures [5–7], and is a candidate for high-temperature structural materials. However, this material contains grain boundaries or colonies between  $\text{Al}_2\text{O}_3$  and YAG, which are expected to impair the mechanical properties. On the other hand, Waku *et al.* [8–11] have recently reported on a unidirectionally solidified  $\text{Al}_2\text{O}_3/\text{YAG}$  eutectic composite manufactured using a eutectic reaction composed of 82 mol %  $\text{Al}_2\text{O}_3$ -18 mol %  $\text{Y}_2\text{O}_3$ , with a

dimension of 10 mm in diameter and 50 mm in height, and made up of a single-crystal  $\text{Al}_2\text{O}_3$  phase and a single-crystal YAG phase containing no colonies or pores. This composite has excellent high-temperature strength characteristics, creep resistance, superior oxidation resistance, and a thermally stable microstructure. Success was also achieved in manufacturing a still larger unidirectionally solidified eutectic composite with a single-crystal  $\text{Al}_2\text{O}_3$ /single-crystal YAG structure, with a dimension of 40 mm in diameter and 70 mm in height, and this composite also had excellent high-temperature strength characteristics and a stable microstructure at very high temperatures [12].

Accordingly, to investigate the possibilities of this composite as a very high temperature-resistant structural material, this research evaluated its major creep characteristics, oxidation resistance characteristics and thermal stability at high temperatures.

## 2. Experimental

### 2.1. Manufacture of raw powders

Using commercially available  $\text{Al}_2\text{O}_3$  powder (AKP-30, produced by Sumitomo Chemical Co., Ltd., Tokyo, Japan) and  $\text{Y}_2\text{O}_3$  powder ( $\text{Y}_2\text{O}_3$ -RU, submicron-type, produced by Shin-Etsu Chemical Co., Ltd., Tokyo, Japan), ball milling was carried out to obtain a homogeneous composite powder slurry. After removing the ethanol and drying the slurry using a rotary evaporator, preliminary melting was performed by high-frequency induction heating to a Mo crucible (50 mm in outer diameter by 200 mm in height by 5 mm in thickness) to obtain an ingot.

### 2.2. Unidirectional solidification

All experiments were performed using the Bridgman-type equipment at the Japan Ultra-high Temperature Materials Research Center. The ingot obtained by preliminary melting was inserted in a Mo crucible (50 mm in outer diameter by 200 mm in height by 5 mm in thickness) set in a vacuum chamber, and a graphite susceptor was heated by high-frequency induction heating. This heated the Mo crucible and performed the melting. After sustaining the high temperature of 2223 K (about 120 K above melting temperature of approximately 2100 K) for 30 minutes, the Mo crucible was lowered at 5 mm an hour, completing the unidirectional solidification experiment.

### 2.3. Sintering

The mixed powders described above were used to perform hot pressing using graphite dies (50 × 70 mm) in a vacuum ( $10^{-2}$  mmHg). The temperature of the hot press was 1973 K, the pressure of the press was 50 MPa, and pressing time was one hour.

### 2.4. Evaluation method

The specimens used in the creep test were selected so that its axial direction was parallel to the solidification

direction. Strain rate control compressive creep tests were carried out on the 3 × 4 × 6 mm specimens. Fig. 1 shows the creep test equipment. The specimen was heated by heating the carbon susceptor using high-frequency induction heating. The test temperatures were 1773, 1873, and 1973 K. The strain rates were  $10^{-4}$ /s,  $10^{-5}$ /s, and  $10^{-6}$ /s. The tests were conducted in an argon atmosphere. The equipment used in the tests was the Japan Ultra-High-Temperature Materials Research Center's high-temperature uniaxial tension-compression and flexural test system (a modified creep and fatigue machine, type 8562 produced by Instron).

The oxidation resistance tests were carried out using a 6 × 6 × 6 mm specimen. After holding the specimen for a fixed period at 1973 K in an air atmosphere, the specimen was tested for changes in its mass. Flexural test samples (3 × 4 × 36 mm) were also heated at 1973 K in an air atmosphere for a prescribed period. The flexural strength of these specimens was measured both at room temperature and at 1973 K following exposure. For a comparison, commercially available sintered SiC and  $\text{Si}_3\text{N}_4$  were subjected to the same tests and measurement.

Structural analysis was performed using the RAD-RB-type X-ray diffraction equipment produced by Rigaku Denki Co., Ltd. High-resolution transmission electron microscopic (HRTEM) observation of the interface of the  $\text{Al}_2\text{O}_3$  and YAG phases was carried out with a JEM-2010 produced by JEOL Ltd., while the EPMA analysis was conducted with a JMX-8621MX by JEOL.

## 3. Results and discussion

### 3.1. Microstructure

Fig. 2 is SEM images showing the microstructure of a unidirectionally solidified eutectic composite and of a sintered composite with the same chemical composition. The white phases in the micrographs are the YAG ( $\text{Y}_3\text{Al}_5\text{O}_{12}$ ), while the black phase is the  $\text{Al}_2\text{O}_3$  from X-diffraction and EPMA analyses results. The unidirectionally solidified eutectic composite contained no colonies or pores, and moreover, also consisted of a single-crystal  $\text{Al}_2\text{O}_3$  with the  $\langle 110 \rangle$  direction parallel to a direction declined by about 14 degrees from the solidification directions, and a single-crystal of YAG with the  $\langle 743 \rangle$  direction parallel to the solidification direction [12]. The sintered composite, on the other hand, was a polycrystalline material with a fine microstructure.

### 3.2. Creep Characteristics

Fig. 3 shows the typical compressive creep deformation curve of a unidirectionally solidified eutectic composite. In all the curves, there is a plateau area showing a steady state creep in which the creep rate is constant with constant stress. Fig. 4 shows the relationship between compressed creep stress and strain rate in a unidirectionally solidified eutectic composite and a sintered composite at test temperatures of 1773, 1873,

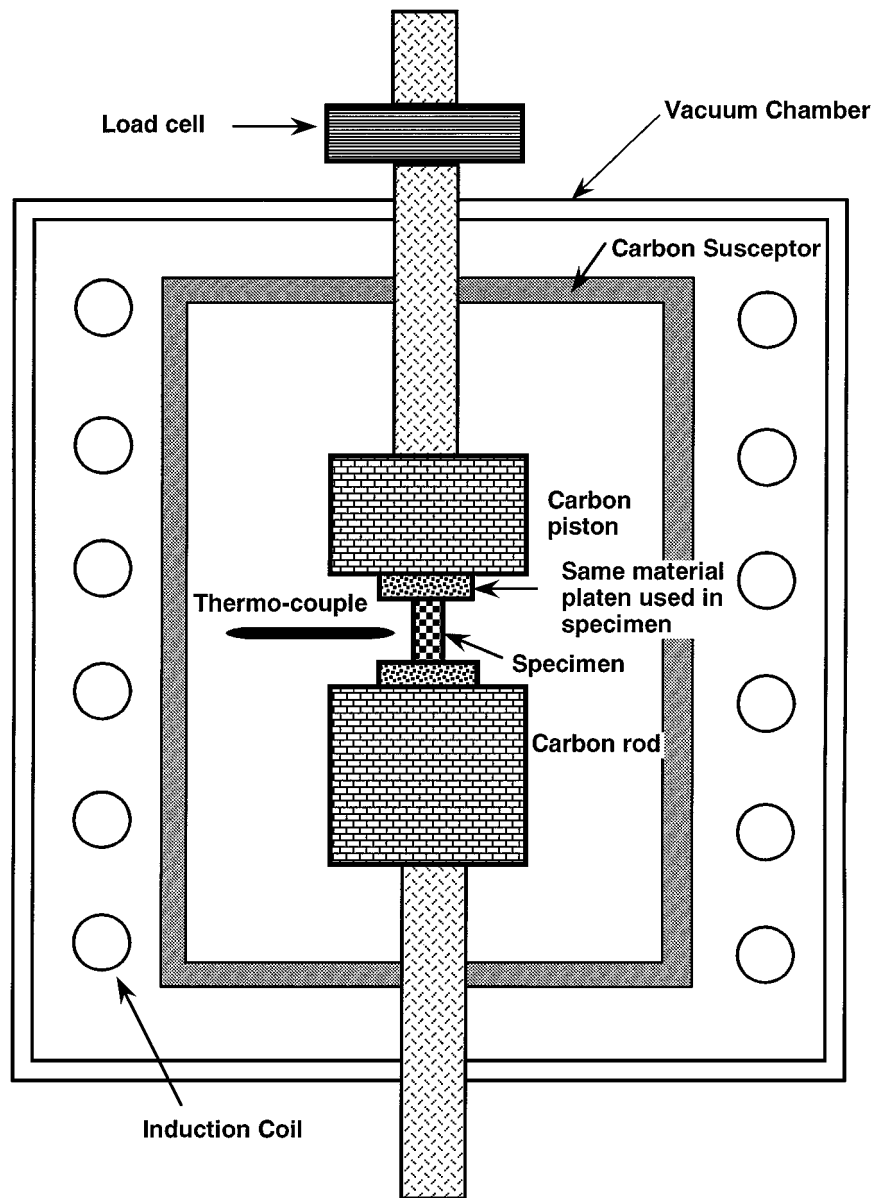


Figure 1 Schematic of compression creep testing apparatus.

and 1973 K. For comparison, data of a polycrystalline YAG [13] are also shown in Fig. 4. While the unidirectionally solidified eutectic composite and the sintered composite shared the same chemical composition and structural phase, their creep characteristics were markedly different. That is, at the same strain rate of  $10^{-4}/s$  and test temperature of 1873 K, the sintered composite showed a creep stress of 33 MPa nearly same as polycrystalline YAG [13], while the unidirectionally solidified eutectic composite's creep stress was approximately 13 times higher at 433 MPa. Moreover, as can be seen from the diagram, the unidirectionally solidified eutectic composite has creep characteristics that surpass those of a-axis sapphire fibers [14] and, as a bulk material, displays excellent creep resistance.

The steady state creep rate  $\dot{\epsilon}$ , can be usually shown by the following equation:

$$\dot{\epsilon} = A\sigma^n \exp(-Q/RT) \quad (1)$$

Here,  $A$ ,  $n$  are dimensionless coefficients,  $\sigma$  is the creep stress,  $Q$  is the activation energy for the creep,  $T$  is the absolute temperature, while  $R$  is the gas constant [15]. In Fig. 4, the value of  $n$  is around 1 for sintered composites, and 5–6 for unidirectionally solidified eutectic composites. As can be seen from the value of  $n$ , the creep deformation mechanism differs according to the manufacturing method. In sintered composites, it can be assumed that the creep deformation mechanism follows the Nabarro-Herring or Coble creep models as shown in polycrystalline YAG [13], while in unidirectionally solidified eutectic composites, the creep deformation mechanism can be assumed to follow the dislocation creep models [15] as shown in reference [7].

Fig. 5 shows the temperature dependence of the steady state creep rate of the unidirectionally solidified eutectic composite, extrapolated from the Fig. 4. It is found that the activation energy for creep is:  $Q = 670\text{--}905$  kJ/mol in agreement with reference [7]. This value falls within the 600–1000 kJ/mol range [15] reported

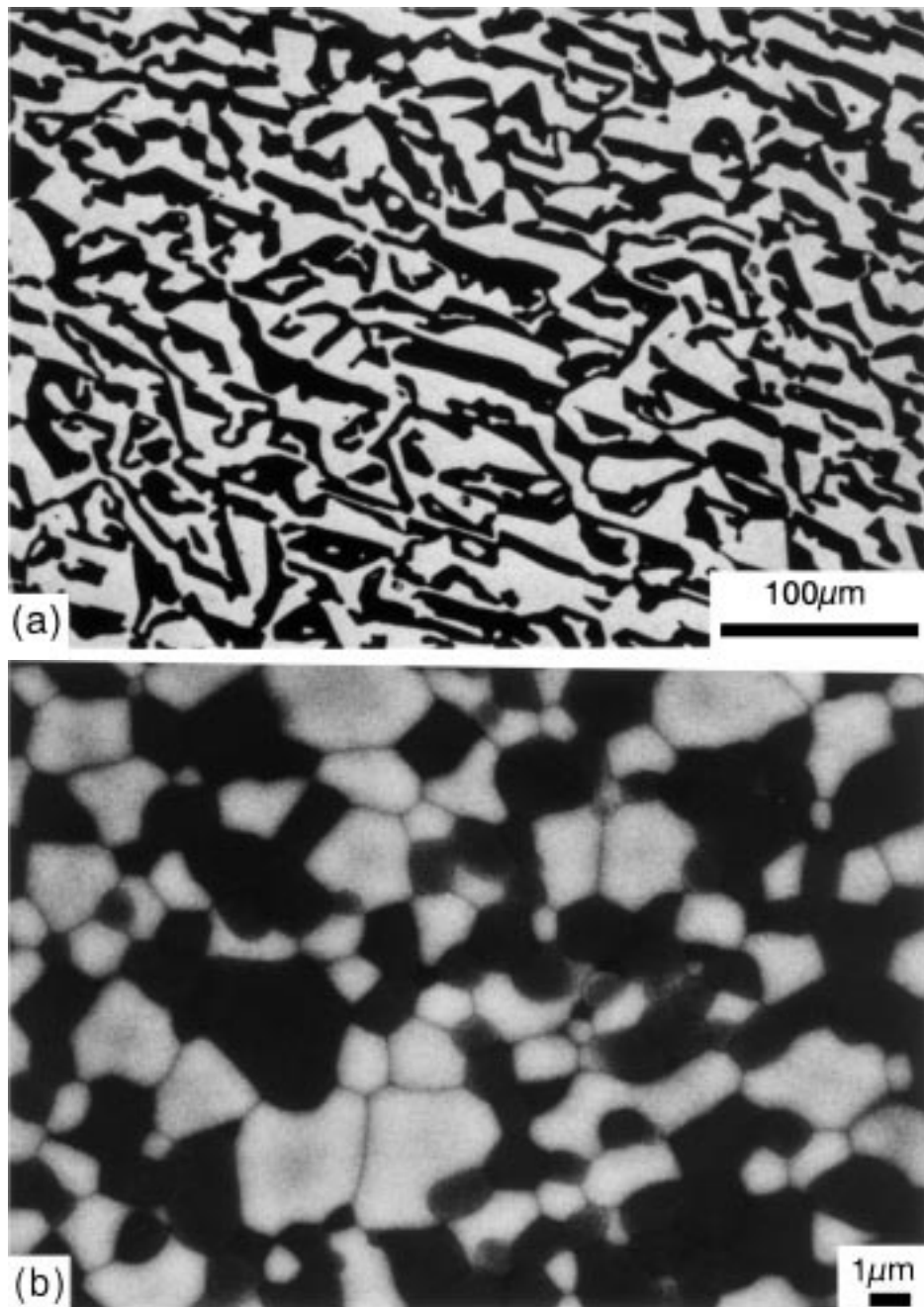


Figure 2 SEM photograph of microstructure of a unidirectionally solidified eutectic composite and a sintered composite: (a) unidirectionally solidified eutectic composite and (b) sintered composite.

for the sapphire, and is wider than the 645–703 kJ/mol range [18] reported for the single-crystal YAG.

As shown in Fig. 6, which shows the results of observing the cross-section microstructure after the creep testing, in the unidirectionally solidified eutectic composite, no voids can be observed in the interface. In the sintered composite, grain growth occurred and voids were observed at the grain boundaries and the triple grain junctions.

The reason that the creep strength and creep deformation mechanism vary according to the manufacturing method even though the chemical composition and the structural phase are the same, is as follows. In high-temperature creep, the diffusion process is dominant, and the poor microstructure is caused by such factors as grain boundaries with active diffusion, and

amorphous phases [15–17]. Because unidirectionally solidified eutectic composites are completely free of these microstructural factors [12], they show excellent creep characteristics. On the other hand, sintered composites have poor creep characteristics because they include grain boundaries and triple grain junctions with amorphous phases [8–12] that are bad for high-temperature creep.

### 3.3. Oxidation resistance

Fig. 7 shows the change in mass of eutectic composites manufactured by the unidirectional solidification method when these eutectic composites are exposed for a fixed period in an air atmosphere at 1973 K. For a comparison, Fig. 7 also shows the results of oxidation

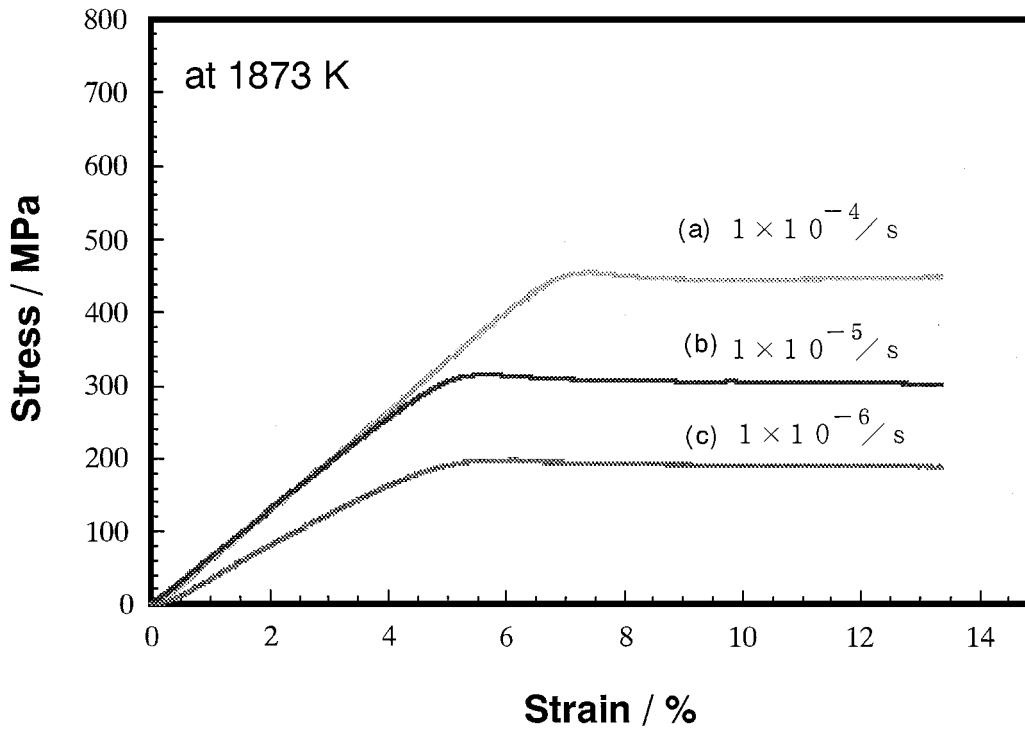


Figure 3 Typical creep deformation curves in a unidirectionally solidified eutectic composite at 1873 K. Strain rates are: (a)  $1 \times 10^{-4}$  /s, (b)  $1 \times 10^{-5}$  /s and (c)  $1 \times 10^{-6}$  /s.

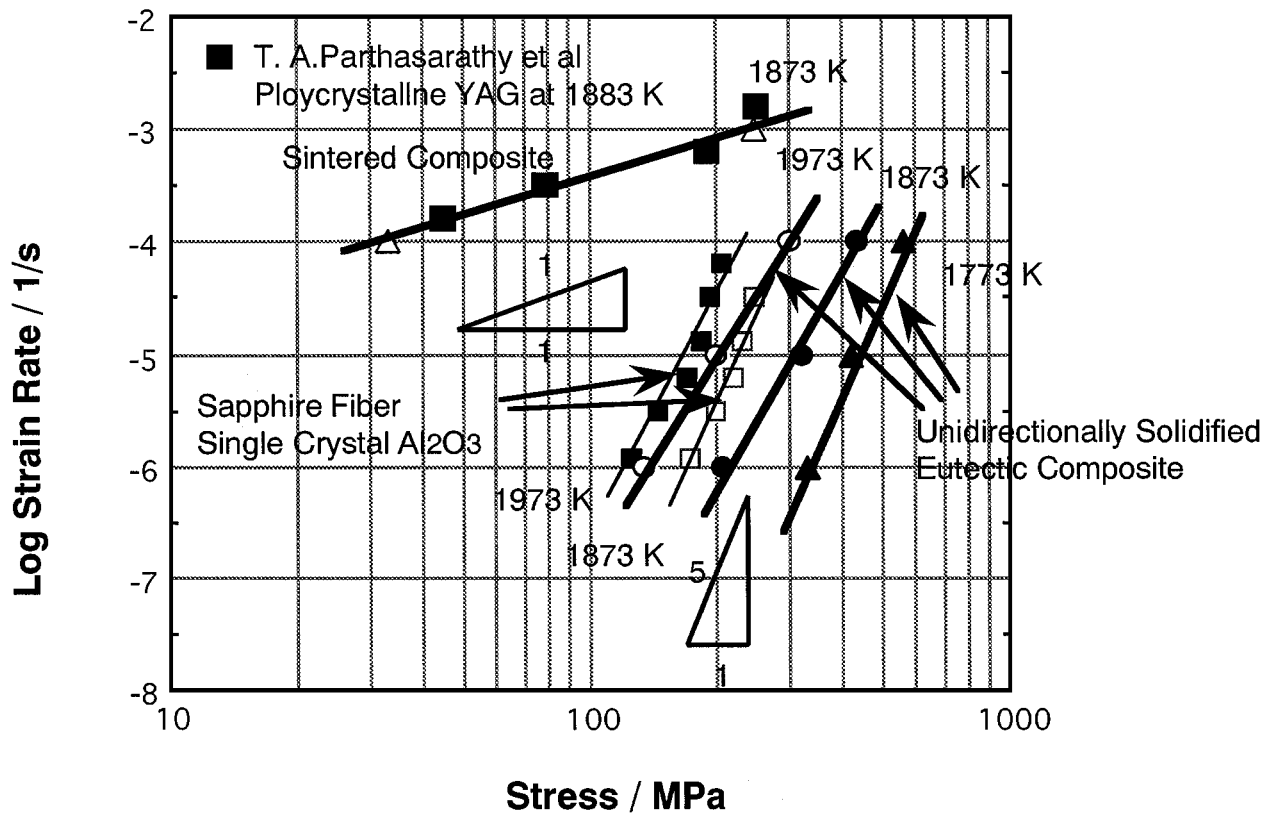


Figure 4 Comparison of compression creep in a unidirectionally solidified eutectic composite and a sintered composite.

resistance tests performed under the same conditions on ceramics SiC and Si<sub>3</sub>N<sub>4</sub>. As the Fig. 7 shows, Si<sub>3</sub>N<sub>4</sub> was shown to be unstable. When it was exposed to 1973 K for 10 hours in the atmosphere, the following reaction took place; Si<sub>3</sub>N<sub>4</sub> + 3O<sub>2</sub> → 3SiO<sub>2</sub> + 2N<sub>2</sub> and the collapse of the shape of the Si<sub>3</sub>N<sub>4</sub> occurred. Likewise,

when SiC was held at 1973 K for 50 hours, it was also shown to be unstable. The following reaction took place; 2SiC + 3O<sub>2</sub> → 2SiO<sub>2</sub> + 2CO and the collapse of the shape also occurred.

On the other hand, when the unidirectionally solidified Al<sub>2</sub>O<sub>3</sub>/YAG eutectic composite was exposed in an

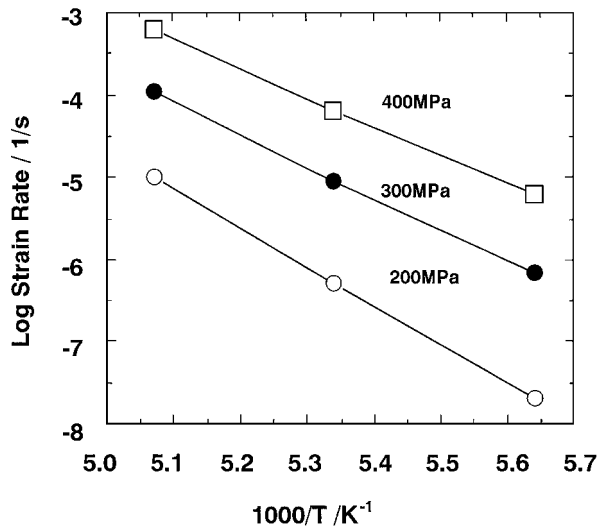


Figure 5 Temperature dependence of steady state creep rate in a unidirectionally solidified eutectic composite.

air atmosphere at 1973 K for 1000 hours, the composite displayed excellent oxidation resistance with no change in mass whatsoever.

Fig. 8 shows the relationship between flexural strength and heat treatment time at 1973 K in an air atmosphere. For comparison, Fig. 8 also shows results for SiC and Si<sub>3</sub>N<sub>4</sub>. When the unidirectionally solidified eutectic composite was tested following exposure, there were no changes in flexural strengths both at room temperature and 1973 K, demonstrating that the composite is an extremely stable material. In contrast, when SiC and Si<sub>3</sub>N<sub>4</sub> were heated to 1973 K in an air atmosphere for only 15 minutes, a marked drop in flexural strength occurred. Fig. 9 shows changes in the surface microstructure of these test specimens before and after heat treatment. There was little difference in surface microstructure of the unidirectionally solidified eutectic composite following 1000 hours of oxidation resistance testing.

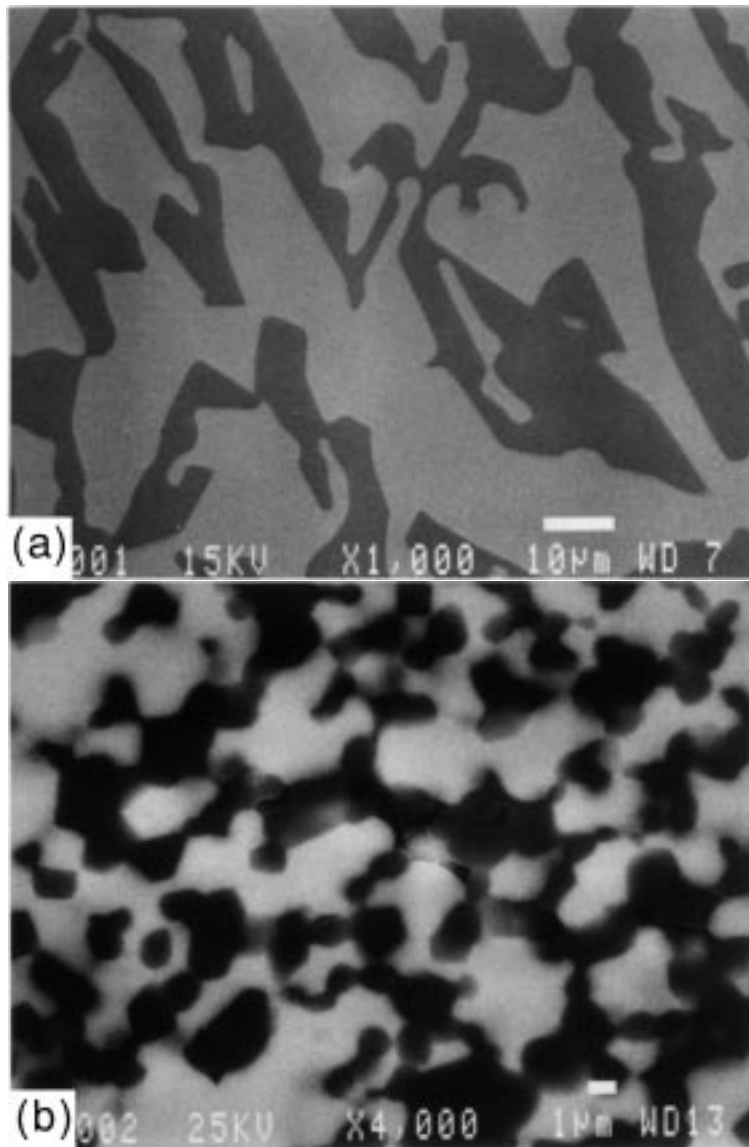


Figure 6 SEM photograph showing the microstructures of a unidirectionally solidified eutectic composite and a sintered composite after compression creep testing at 1873 K: (a) unidirectionally solidified eutectic composite and (b) sintered composite.

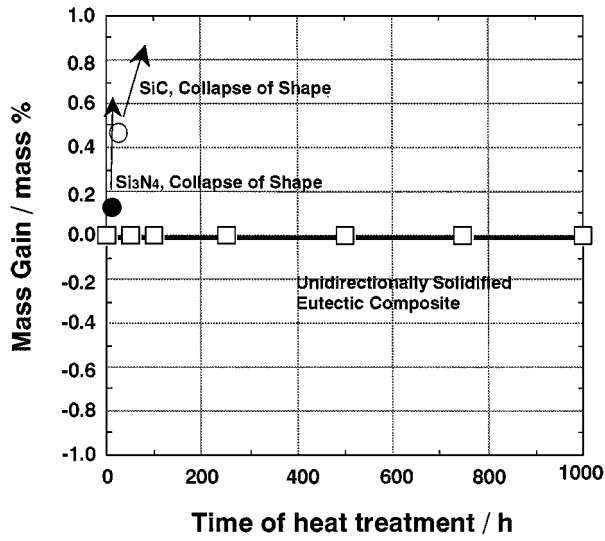


Figure 7 Comparison of oxidation resistance characteristics of a unidirectionally solidified eutectic composite and advanced ceramics SiC and Si<sub>3</sub>N<sub>4</sub> at 1973 K in an air atmosphere.

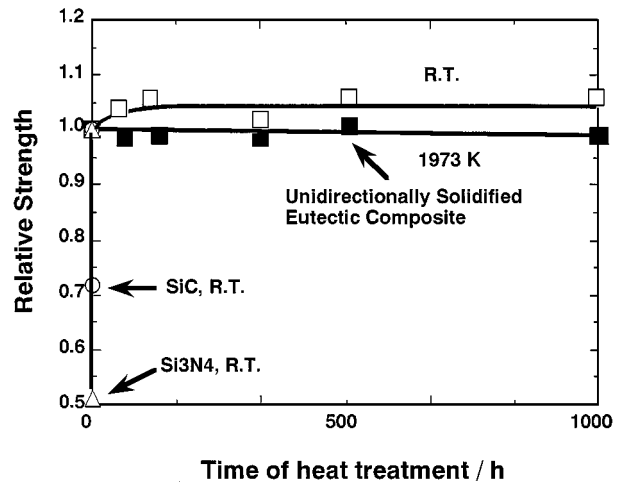


Figure 8 Changes caused by length of heating in relative strength of unidirectionally solidified eutectic composites and advanced ceramics SiC and Si<sub>3</sub>N<sub>4</sub> at room temperature at 1973 K. The relative strength is the ratio of flexural strength after a prescribed period of heating in an air atmosphere at 1973 K to as-received flexural strength.

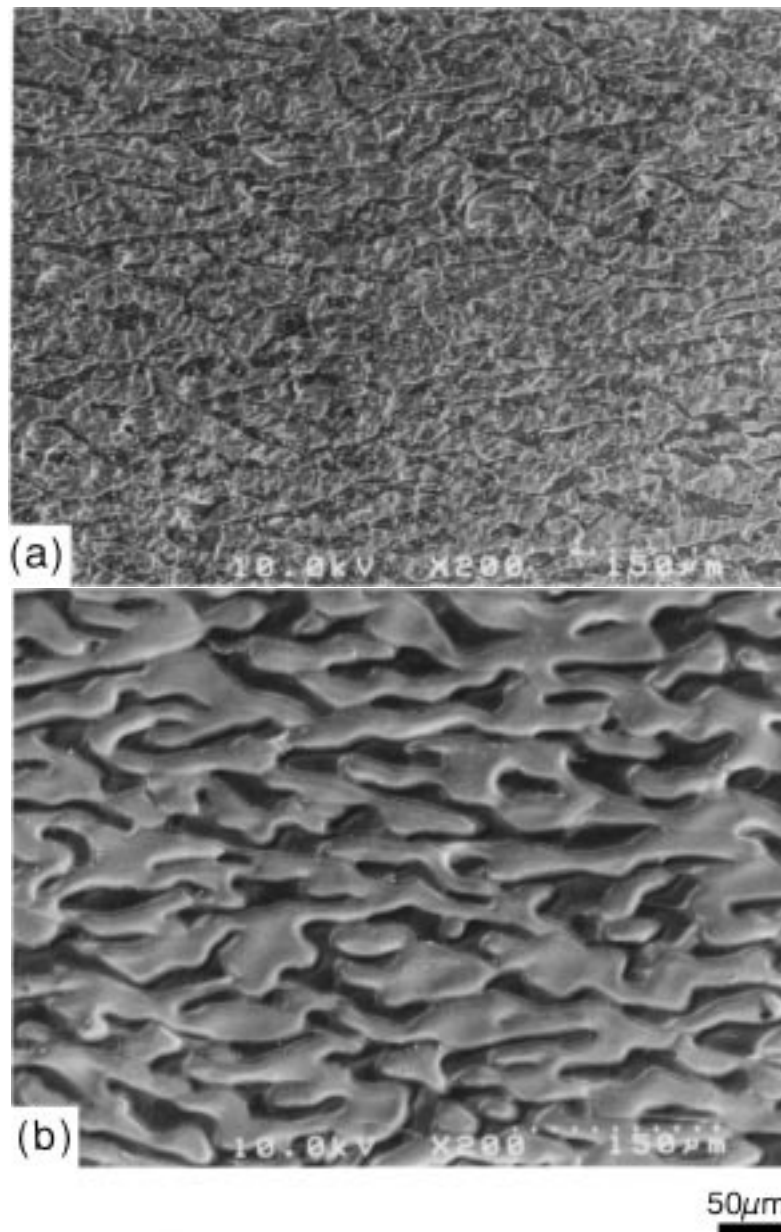


Figure 9 SEM images of surface microstructure before and after oxidation resistance testing at 1973 K in air for 1000 h: (a) the pre-test surface microstructure of the unidirectionally solidified eutectic composite and (b) post-test surface microstructure.

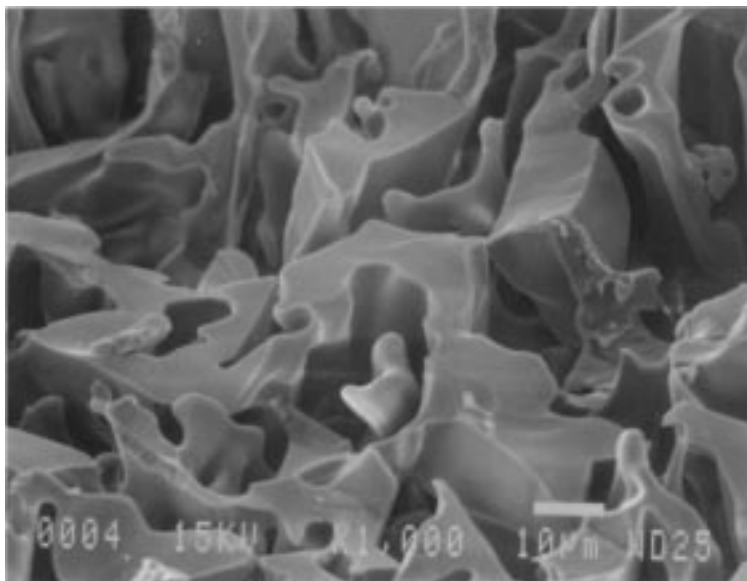


Figure 10 SEM observation of the three-dimensional structure of the YAG phase.

### 3.4. Three-dimensional shape of compositional microstructure of unidirectionally solidified composites

As shown above, eutectic composites manufactured by unidirectional solidification are highly likely to remain stable under use in an air atmosphere at temperatures in excess of 1923 K. This kind of high-temperature performance is closely related to the composite microstructure with the previously mentioned lack of grain boundaries, formation of interfaces with comparatively good coherency because of the absence of amorphous phases, and three-dimensional single-crystal  $\text{Al}_2\text{O}_3$ /single-crystal YAG phases. Fig. 10 is a SEM photograph of the three-dimensional YAG phase with only the  $\text{Al}_2\text{O}_3$  phase excluded, after the eutectic composite was heated in graphite powder for two hours at 1973 K. As the photograph clearly shows, the YAG phase is three-dimensionally linked, extremely complex, having a hieroglyphic-like configuration. In other words, the single-crystal  $\text{Al}_2\text{O}_3$  and the single-crystal YAG are linked three dimensionally to form a complex, interlocking structure. As a result, coupled with crystallographic characteristics and compatible interfaces, the eutectic composite has prolonged stability at 1973 K, and manifests excellent creep characteristics and thermal stability.

### 4. Conclusions

Employing unidirectional solidification, a  $40\phi \times 70$  mm eutectic composite with a single-crystal  $\text{Al}_2\text{O}_3$ /single-crystal YAG structure was manufactured successfully, and its creep characteristics and its thermal stability were evaluated.

The compressed creep resistance of the unidirectionally solidified eutectic composite was about 13 times higher than a sintered composite with the same chemical composition and structural phases. While the stress exponent,  $n$ , for the sintered composite was about 1,

that for the unidirectionally solidified eutectic composite was 5–6. The activation energy for the steady state creep of the unidirectionally solidified eutectic composite was around 670–905 kJ/mol. After 1000 hours at 1973 K in an air atmosphere no change whatsoever was observed in the highly stable eutectic composite's mass. These excellent high-temperature characteristics of the unidirectionally solidified eutectic composite are closely linked to such factors as: (1) the composite consisting of a single-crystal  $\text{Al}_2\text{O}_3$  phase and single-crystal YAG phase with no grain boundaries, (2) interfaces with comparatively good coherency and no amorphous phases are formed, (3) the phases being connected three-dimensionally and having a complex interlocking structure.

### References

1. *The Japan Industrial Journal*, September (1994) 6.
2. E. L. COURTRIGHT, H. C. GRAHAM, A. P. KATZ and R. J. KERANS, "Ultrahigh temperature assessment study-ceramic matrix composites." Materials Directorate, Wright Laboratory, Air Force Materiel Command, Wright-Patterson Air Force Base (1992) 1.
3. WILLIAM B. HILLING, Prospects for ultrahigh-temperature ceramic composites, in "Tailoring Multiphase and Composite Ceramics," edited by Richard E. Tressler, Gray L. Messing, Carlo G. Pantano, and Robert E. Newnham (Plenum Press, New York). *Mater. Sci. Res.* **20** (1986) 697–712.
4. D. VIECHNICKI and F. SCHMID, *J. Mater. Sci.* **4** (1969) 84.
5. T. MAH and T. A. PARTHASARATHY, *Ceram. Eng. Sci. Proc.* **11** (9/10) (1990) 1617.
6. T. A. PARTHASARATHY, T. MAH and L. E. MATSON, *ibid.* **11** (9/10) (1990) 1628.
7. T. A. PARTHASARATHY, MAR, TAI-II and L. E. MATSON, *J. Amer. Ceram. Sci.* **76** (1) (1993) 29.
8. Y. WAKU, N. NAKAGAWA, H. OHTSUBO, Y. OHSORA and Y. KOHTOKU, *J. Japan Inst. Metals* **59**(1) (1995) 71.
9. Y. WAKU, H. OHTSUBO, N. NAKAGAWA and Y. KOHTOKU, *J. Mater. Sci.* **31** (1996) 4663.
10. Y. WAKU, N. NAKAGAWA, H. OHTSUBO and Y. KOHTOKU, in Proceeding of the 16th International SAMPE



- Europe Conference of the Society for the Advancement of Material and Process Engineering, Salzburg, Austria, May–June, (1995) p. 117.
11. Y. WAKU, in Proceedings of the Ninth Symposium on Ultra-High Temperature Materials, Ube, Japan, June (1995) p. 52.
  12. Y. WAKU, N. NAKAGAWA, T. WAKAMOTO, H. OHTSUBO, K. SHIMIZU and Y. KOHTOKU, *J. Mater. Sci.* **33** (1998) 1217.
  13. T. A. PARTHASARATHY, T. MAH and K. KELLER, *J. Amer. Ceram. Soc.* **75** (1992) 1756.
  14. D. M. KOTCHICK and R. E. TRESSLER, *ibid.* **63** (1980) 429.
  15. W. R. CANNOM and T. G. LAGDON, *J. Mater. Sci.* **18** (1983) 1.
  16. D. R. CLARKE, *J. Amer. Ceram. Soc.* **62** (1979) 236.
  17. J. ECHIGOYA, S. HAYASHI, K. SASAKI and H. SUTO, *J. Japan Inst. Metals* **48** (1984) 430.
  18. G. S. CORMAN, “Creep of Oxide Single Crystals,” U.S. Air Force Contract No. F33615-87-C-5354 Final Technical report No. WRDC-TR-90-4059, August, 1990.

*Received 20 February 1997  
and accepted 18 September 1998*